PERGAMON

Scripta Materialia 47 (2002) 69–76

Scripta MATERIALIA

www.actamat-journals.com

Nanoscale crystallographic analysis of ultrafine grained IF steel fabricated by ARB process

N. Tsuji *, R. Ueji, Y. Minamino

Department of Adaptive Machine Systems, Graduate School of Engineering, Osaka University, 2-1 Yamadaoka, Suita, Osaka 565-0871, Japan

Received 19 February 2002; received in revised form 12 March 2002; accepted 5 April 2002

Abstract

Nanoscale crystallographic features of ultrafine grained interstitial free steel fabricated by accumulative roll-bonding (ARB) process have been studied by electron back-scattered diffraction in field-emission type scanning electron microscope. This work has clearly indicated that most of the elongated ultrafine grains in the ARB processed sheet are surrounded by high-angle grain boundaries. The characteristic textures in the ARB processed sheet were also clarified. © 2002 Acta Materialia Inc. Published by Elsevier Science Ltd. All rights reserved.

Keywords: Steel; Electron diffraction; Grain boundaries; Ultrafine grains; Texture

1. Introduction

It has been shown recently that intense straining of metallic materials can produce ultrafine grained microstructure with the mean grain size smaller than 1 μm [1]. Various intense straining processes have been proposed for ultra grain refinement, such as accumulative roll-bonding (ARB) [2], equal channel-angular extrusion [3], etc., and these processes have actually succeeded in producing ultrafine grained metallic materials in a bulk form [2–10]. Nevertheless, the definition of the ''ultrafine grains'' formed by intense straining is still not clear, since fine subgrains or dislocation cells surrounded by low-angle boundaries can be formed by heavy deformation as well. However, ultrafine grains should be distinguishable from subgrains or cells, because the difference in misorientation (high-angle or low-angle) of the boundaries largely affects the properties of the materials, such as strength, toughness, superplasticity, etc. It is, therefore, essential to clarify whether the grain boundaries of the obtained ultrafine grains are high-angle or low-angle. However, quantitative studies of the crystallography of ultrafine grained materials are still limited, although some researchers have reported detailed misorientation maps in relatively small areas [8–12]. In the present study, the crystallographic analysis of the ultrafine grained steel has been attempted by an electron back-scattered diffraction (EBSD) technique [13] in a field-emission type scanning electron microscope (FE-SEM), which is the only possible tool for nanoscale analysis of relatively large areas at present [14,15].

* Corresponding author. Tel.: +81-6-6879-7434; fax: +81-6-6879-7570.

E-mail address: tsuji@ams.eng.osaka-u.ac.jp (N. Tsuji).

1359-6462/02/$ - see front matter
PII: S1359-6462(02)00088-X

2. Experimental

ARB of a Ti-added ultra-low carbon interstitial free (IF) steel was carried out in the same way as reported previously [6]. The chemical composition of the IF steel is shown in Table 1. The initial sheets had a polygonal ferrite microstructure with the mean grain size of 23 μm. Two pieces of the sheets 1 mm in thickness, 30 mm in width and 300 mm in length were stacked to be 2 mm thick after surface treatment (degreasing and wire-brushing), kept in an electrical furnace at 773 K for 600 s, and then roll-bonded by 50% reduction (equivalent strain; $\varepsilon = 0.8$) in one pass by the use of a two-high mill with a roll diameter of 310 mm. The roll-bonded sheet was immediately cooled in water and cut into two pieces. Such a procedure was repeated for up to 5 cycles ($\varepsilon = 4.0$).

Thin foils parallel to the transverse direction (TD) of the ARB processed sheet were prepared for TEM observation by twin-jet electropolishing in a 100 ml $HClO_4$ + 900 ml CH_3COOH solution. Hitachi H-800 microscope was operated at 200 kV. EBSD orientation mapping was done on a longitudinal section perpendicular to TD of the sheet. The measured section was located at the center of the width in the sheet. The specimen was electropolished in the same solution as that for thin foil preparation. The EBSD measurements were carried out using a program developed by TSL Inc. (OIM™) in Phillips XL30S SEM equipped with FE-gun operated at 15 kV. Orientation mapping with a step size of 50 nm was carried out over 10 μm × 50 μm areas near the center of the thickness and just below the sheet surface. As a result, about 230,000 orientations were analyzed for each area.

3. Results

Fig. 1 shows a TEM microstructure and corresponding selected area diffraction (SAD) pattern

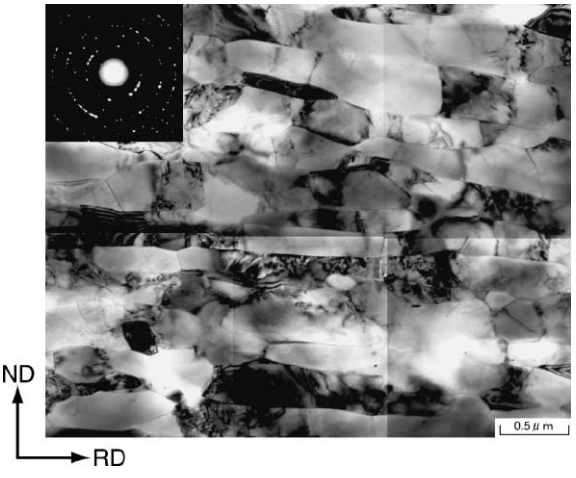

Fig. 1. TEM micrograph and corresponding SAD pattern of the IF steel sheet ARB processed by five cycles ($\varepsilon = 4.0$) at 773 K. Observed from TD near the thickness center of the sheet.

of the specimen ARB processed by five cycles ($\varepsilon = 4.0$) at 773 K. The microstructure was observed near the center of the thickness of the sheet. An elongated ultrafine grained microstructure was observed. This is a typical view of the pancake-shaped ultrafine grains produced by ARB [7–10]. The mean grain thickness and length of the ultrafine grains are 210 and 700 nm, respectively. There were some dislocations and sub-boundaries within the elongated ultrafine grains, but the number of dislocations seems small for a highly strained material. The diffraction pattern was taken by the use of an aperture 4.4 μm in diameter. The SAD pattern indicates that a number of different orientations exist within the small area. This method has been the "conventional" method used to justify the presence of the large misorientations of the ultrafine grained microstructure, as will be discussed later.

Fig. 2(a) is a macroscopic view of the specimen in SEM. Some of the bonded boundaries, especially the latest bonded one at center, in the ARB processed sheets are severely etched by electropolish-

Table 1
Chemical composition of the IF steel studied (mass%)

C	N	Si	Mn	P	Cu	Ni	Ti	Fe
0.002	0.003	0.01	0.17	0.012	0.01	0.02	0.072	Bal.

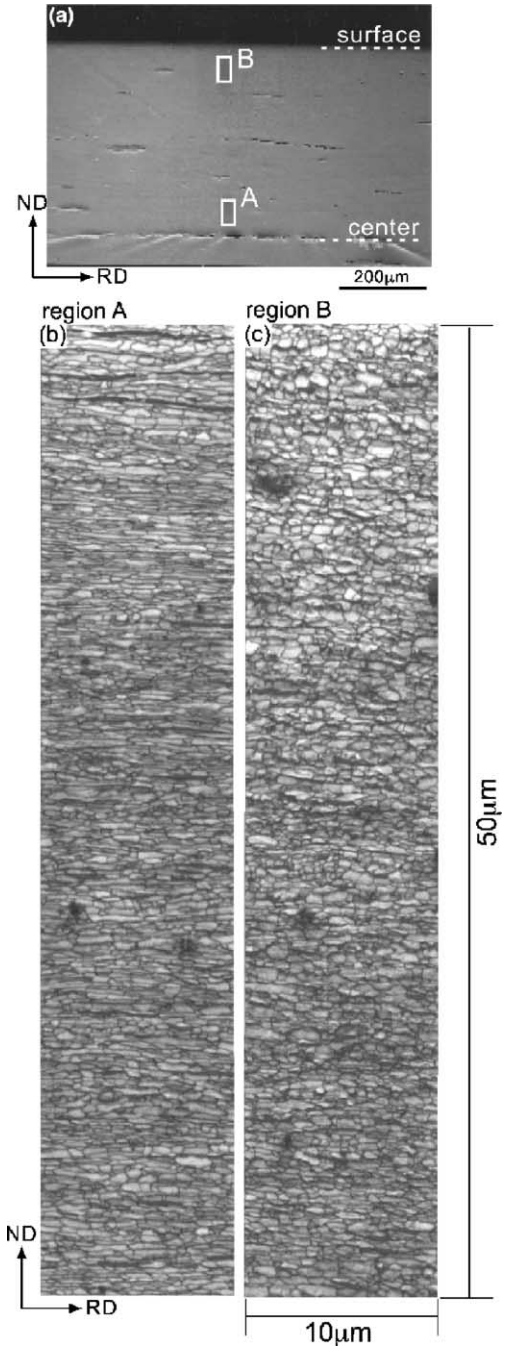

Fig. 2. SEM micrograph (a) of the ARB processed IF steel and IQ maps of the regions A (b) and B (c) obtained by EBSD measurement in FE-SEM.

ing and show the grooves. The two different areas represented by white rectangles in Fig. 2(a) were analyzed by EBSD. Hereafter, they are referred to as region A (center region) and region B (surface region). Fig. 2(b) and (c) are the maps of the regions A and B, respectively, constructed by the image quality (IQ) of the Kikuchi-lines. Sound Kikuchi-lines were obtained from most of all the area even in the present heavily deformed samples. The average IQ and confidence index (CI) values in OIM™ software were 94.3 and 0.54 for the region A, and 95.1 and 0.52 for the region B, respectively. It was hard to obtain sound Kikuchi-lines from the same sample in a conventional SEM equipped with LaB_6 filament. This demonstrates the usefulness of FE-SEM for the ultrafine microstructures. The IQ of Kikuchi-line decreases near or just on lattice defects, such as dislocations, subboundaries and grain boundaries, so that these points have dark contrast in the IQ maps. As a result, the elongated ultrafine grains are well reconstructed in Fig. 2(b) and (c). The ultrafine grains in the region B, especially those close to the surface, are more equiaxed than those in the region A.

Figs. 3 and 4 show the orientation maps of the regions A and B. Figures (a) and (b) are the color maps showing ND and RD orientations, respectively. The correspondence between the colors and the crystal orientations is represented in the stereographic triangles in Figs. 3 and 4. Fig. 3(a) shows wide variety of colors, while colors close to green dominate in Fig. 3(b). This indicates that the region A (center region) has RD//$\langle 1\,1\,0\rangle$ texture, which is known as α-fiber texture in rolled bcc metals [16]. However, there are scarcely colonies with the same color (orientation) in the ND color map. On the other hand, the tendency of the colors in Fig. 4(a) and (b) is completely different from Fig. 3. Green colors dominate the ND color map of the region B (Fig. 4(a)) and the red and purple colors are the majority in the RD color map (Fig. 4(b)). The results mean that the surface region has the $\{1\,1\,0\}\langle 0\,0\,1\rangle \sim \{1\,1\,0\}\langle 1\,1\,2\rangle$ texture. This can be considered as a kind of shear texture, as will be discussed later. Figs. 3(c) and 4(c) show boundary misorientation maps. Before constructing the boundary maps, the measured points whose CI values were smaller than 0.1 were removed to increase reliability of the analysis. The eliminated points are painted black in the figures, as "bad

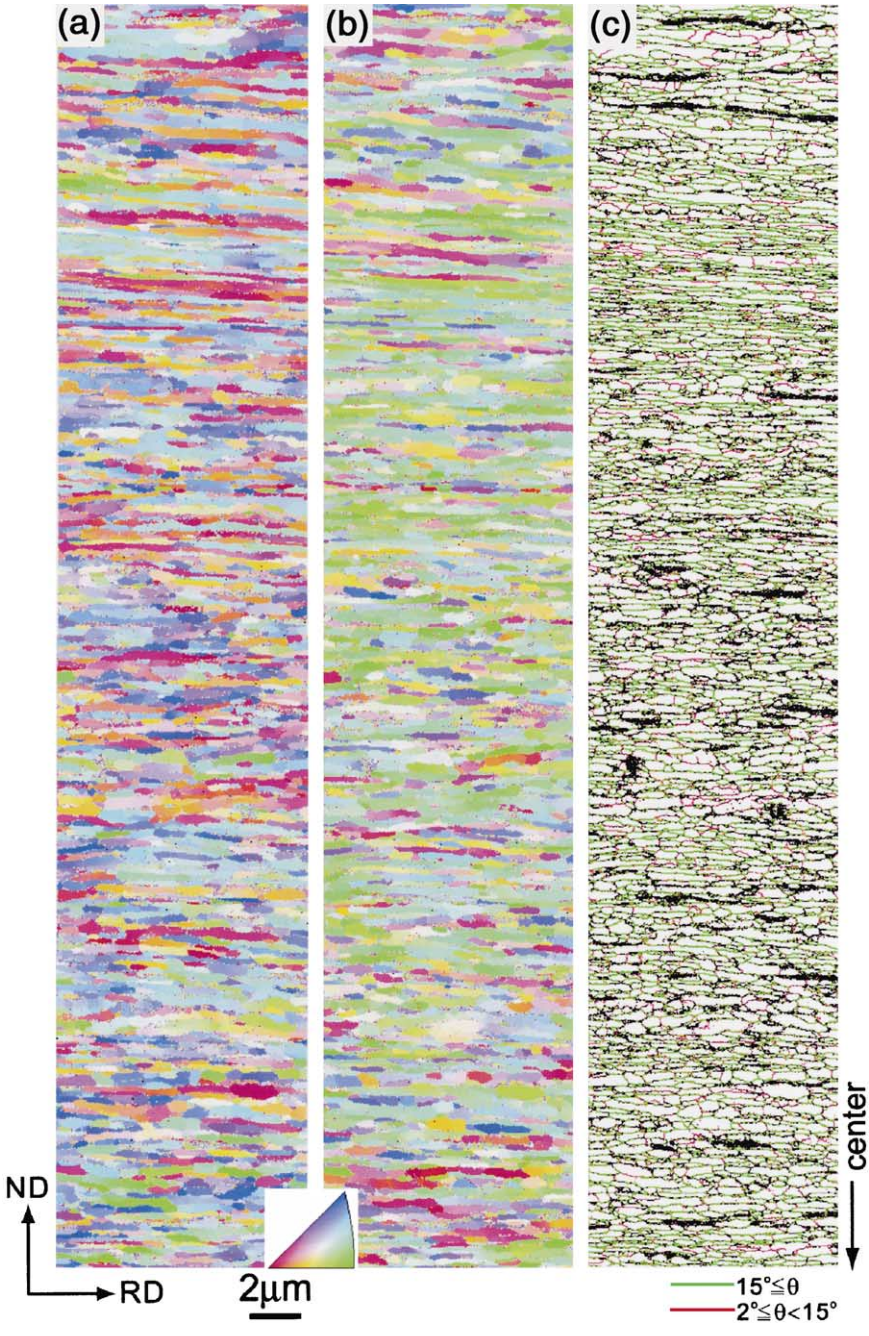

Fig. 3. Orientation imaging microstructures of the region A (near center) obtained by EBSD measurement. (a) ND orientation color map, (b) RD orientation color map, (c) boundary misorientation map.

points'' where accurate orientation analysis failed. After this procedure, the green lines were drawn when the misorientation between the adjacent points was larger than 15°. That is, the green lines

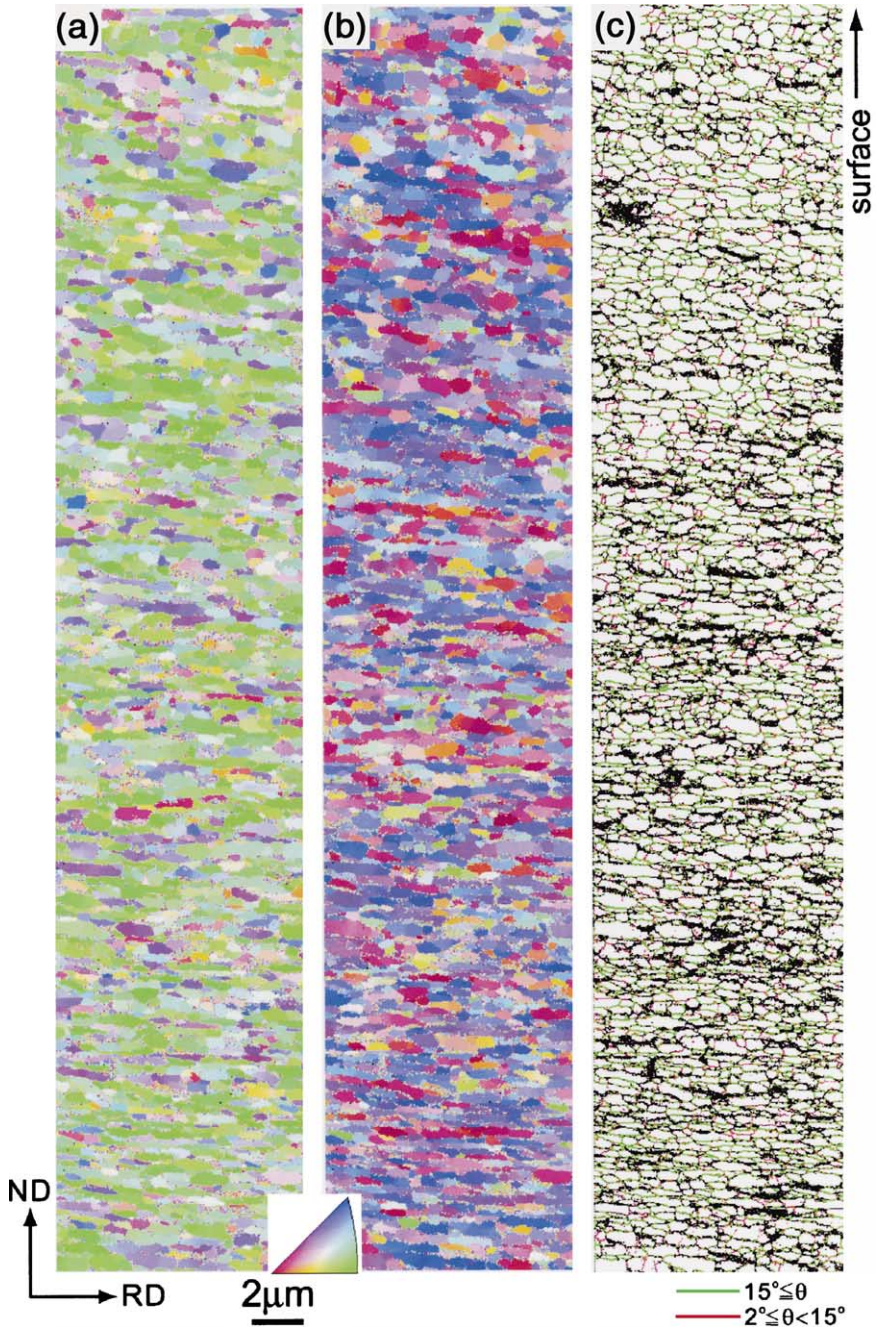

Fig. 4. Orientation imaging microstructures of the region B (near surface) obtained by EBSD measurement. (a) ND orientation color map, (b) RD orientation color map, (c) boundary misorientation map.

in Figs. 3(c) and 4(c) correspond to high-angle grain boundaries. On the other hand, the red lines were drawn as low-angle boundaries, when the misorientation was smaller than 15° and larger

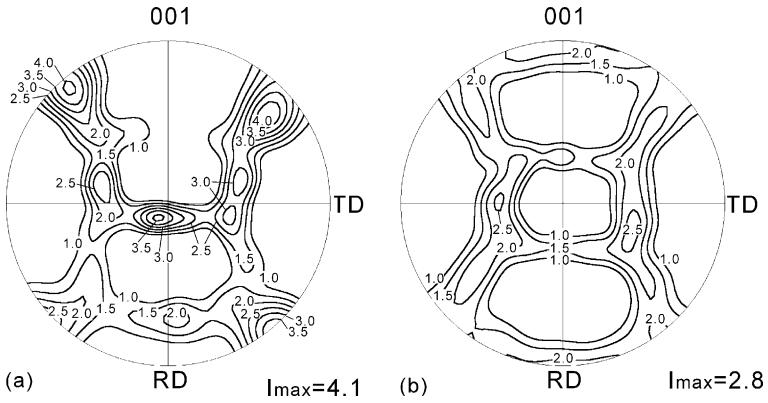

Fig. 5. {1 0 0} pole figures of the regions A (a: near center) and B (b: near surface) constructed from the EBSD data.

than 2°. The lower boundary criterion of 2° was chosen because 1.5° criterion made too many red lines (low-angle boundaries) compared with the previous TEM map [8], which must include the error in EBSD measurement. Most of the ultrafine grains in the both regions are surrounded by high-angle grain boundaries, although many low-angle boundaries are also included in the microstructures. Especially, almost all the boundaries parallel to RD are high-angle ones. Such results are consistent with the previous results about orientation analysis of the relatively small areas in TEM [7–10]. However, the number of the low-angle boundaries in Figs. 3(c) and 4(c) is much smaller than that reported in TEM/Kikuchi-line analysis [7–10]. This is because misorientations smaller than 2° were neglected in the present analysis. This means that the EBSD mapping is not so suitable for reconstructing real low-angle boundaries or dislocation substructures. Nevertheless, it can be concluded that the elongated ultrafine grains obtained by ARB process are not subgrains but "grains" having large misorientations to each other.

The {1 0 0} pole figures of the both regions are shown in Fig. 5. The large difference in texture between the surface and the center can be clearly recognized. The center region has some similarity to the typical rolling texture of bcc iron and ferritic steels with an α-fiber [16], though it is somewhat asymmetric across the ND–TD plane. On the other hand, near the surface $\{110\}\langle001\rangle$ and $\{110\}\langle112\rangle$ orientations suggested from the color maps (Fig. 4(a) and (b)) are seen in Fig. 5(b). This is similar to the pole figure reported in the surface sheared regions in hot-rolled steels [17].

4. Discussion

In this work, the nanoscale crystallographic features of the ultrafine grained microstructure produced by intense straining have been clarified in macroscopic views by EBSD analysis. Most the previous researchers studying severely deformed materials have insisted that the obtained ultrafine grains have large misorientations to each other on the grounds of the ring-like or circumferentially spread diffraction patterns seen in TEM [2,3], like Fig. 1. However, SAD method cannot be a quantitative way for misorientation measurement. Furubayashi [18] has pointed out the inaccuracy in orientation determination by SAD. Further, Mishin et al. [19] has assessed the SAD method for misorientation measurement and clearly concluded that the azimuth spread in SAD pattern can only reflect the orientation spread within a specific area qualitatively and it should not be classified as the boundary misorientation. Therefore, the SAD method is not appropriate for discussing the detailed crystallographic features of the ultrafine grains, especially grain boundary characters. In order to characterize the boundaries, it is necessary to obtain an accurate orientation for each ultrafine grain. Tsuji et al. [7–10] tried precise crystal-

lographic analysis of the ultrafine grained microstructures in IF steel and aluminum ARB processed by means of convergent beam Kikuchi-line analysis in TEM, and showed that the pancake-shaped ultrafine grains are surrounded by high-angle grain boundaries with misorientations larger than 15°. Belyakov et al. [11,12] also reported the high density of high-angle boundaries within the ultrafine grained microstructure of austenitic stainless steel and copper severely deformed by multiaxial compression after Kikuchi-line analysis. However, still such measurements in TEM have been limited to small areas and macroscopic information including statistical texture data for the ultrafine grains have not yet been widely represented. The present trial clearly demonstrated that EBSD in FE-SEM can be a strong tool for nanoscale crystallographic analysis of relatively large areas. It was rather surprising that almost perfect analysis could be performed even in specimens produced by an intense straining process. This method is especially effective in determining the grain boundary character as well as the microscale textures. On the other hand, this method is not so suitable for identifying dislocation substructures and sub-boundary structures, as was shown in the fact that the number of the low-angle boundaries drawn in the boundary maps (Figs. 3(c) and 4(c)) depends on the lower-boundary criterion in the analysis. This is reasonable because the orientation map by EBSD is essentially constructed by inserting information between the discrete points of the measurement. Anyway, it has been proved in large area views that the elongated ultrafine grains produced by ARB are not subgrains but are "grains" having large misorientations to each other. In the sense of boundary misorientation, therefore, it can be said that the ultrafine grains have the character of recrystallized grains. On the other hand, the ultrafine grains have the elongated morphology and the dislocation substructures inside, which is a characteristic of a deformed microstructure. These features throw more light on the formation mechanism of the ultrafine grains during intense straining [20] which has not yet been fully clarified.

The present study has also shown that the texture is largely different between center and subsurface. The difference can be understood from a viewpoint of shear deformation during rolling. The rolling (roll-bonding) in the present ARB was carried out without any lubricant, because rolling under high-friction condition accelerates the strengthening and ultrafine grain formation in ARB [21]. Under such condition, large amount of shear strain is introduced near the surface of the sheet due to large friction between the material and the rolls [17]. The distribution of the shear strain is quite complex in the ARB processed sheet, as was quantitatively shown by Lee et al. [22], since the procedure of roll-bonding, cutting and stacking is repeated in ARB. However, the surface in the final sheet has been always surface during the ARB, so that it is reasonable that the region B has a kind of shear texture owing to accumulation of the redundant shear strain. It is interesting that the region A is similar to the typical rolling texture, because the center had been the surface until the fourth cycle of the ARB. The result suggests that the shear texture can be easily destroyed by conventional rolling deformation in the fifth cycle. The asymmetry of Fig. 5(a) probably reflect such a transition of the texture. The texture effect might be one of the keys to understand the formation mechanism of the ultrafine grains in ARB, in other words, the ultrafine grain subdivision [20,23]. Therefore in the future, a more detailed examination should be carried out concerning the relationship between the texture and the shear strain distribution [22] in the ARB processed materials in the next step.

5. Conclusions

Nanoscale crystallographic characterization of the ultrafine grained microstructure produced by an intense straining process (ARB) was successfully carried out in macroscopic views by the aid of FE-SEM/EBSD technique. The FE-SEM/EBSD technique was quite useful for the orientation analysis of the ultrafine grains or the intensely deformed materials. It was clarified that the ultrafine grains in the IF steel ARB processed up to a strain of 4.0 at 773 K are not subgrains but grains surrounded by high-angle grain boundaries. The ultrafine grains in the as-ARB processed specimen have the features

of both deformed microstructure and recrystallized grains. The region near the thickness center had RD//⟨1 1 0⟩ texture similar to the conventional rolling texture, while the region near the surface of the sheet showed a kind of shear texture.

Acknowledgements

The EBSD measurement in FE-SEM was performed at Kobelco Research Institute Inc. This work was financially supported by Industrial Technology Research Grant Program in '01 from New Energy and Industrial Technology Development Organization (NEDO) of Japan (project ID 01A23025d) and steel research grant from the Iron and Steel Institute of Japan (ISIJ). These supports are gratefully appreciated. The authors also would like to thank Dr. Y. Koizumi of Osaka University and Mr. T. Toyoda, a graduate student of Osaka University, for their help in experiments and discussion.

References

[1] Shaw LL. J Met 2001;52:41.
[2] Saito Y, Utsunomiya H, Tsuji N, Sakai T. Acta Mater 1999;47:579.
[3] Nemoto M, Horita Z, Furukawa M, Langdon TG. Met Mater 1998;4:1181.
[4] Saito Y, Tsuji N, Utsunomiya H, Sakai T, Hong RG. Scripta Mater 1998;39:1221.
[5] Tsuji N, Saito Y, Utsunomiya H, Tanigawa S. Scripta Mater 1999;40:795.
[6] Tsuji N, Shiotsuki K, Saito Y. Mater Trans JIM 1999;40:765.
[7] Tsuji N, Saito Y, Utsunomiya H, Sakai T. In: Mishra RS, Semiatin SL, Suryanarayana C, Thadhani NN, Lowe TC, editors. Ultrafine grained materials. Pennsylvania: TMS; 2000. p. 207.
[8] Tsuji N, Ueji R, Saito Y. Mater Jpn 2000;39:961.
[9] Ito Y, Tsuji N, Saito Y, Utsunomiya H, Sakai T. J Jpn Inst Met 2000;64:429.
[10] Huang X, Tsuji N, Hansen N, Minamino Y. Mater Sci Eng A, in press.
[11] Belyakov A, Sakai T, Miura H, Kaibyshev R. ISIJ Int 1999;39:592.
[12] Belyakov A, Gao W, Miura H, Sakai T. Metall Mater Trans A 1998;29A:2957.
[13] Schwartz AJ, Kumar M, Adams BL, editors. Electron backscatter diffraction in materials science. New York: Kluwer Academic/Plenum Publishers; 2000.
[14] Bowen JR, Prangnell PB, Humphreys FJ. Mater Sci Technol 2000;16:1246.
[15] Prangnell PB, Bowen JR, Gholinia A. In: Proc. of the 22nd RISØ Int. Symp. on Mater. Sci. RISØ National Laboratory, Roskilde, Denmark. 2001. p. 105.
[16] Humphreys FJ, Hatherly M. Recrystallization and related annealing phenomena. New York: Pergamon; 1995.
[17] Sakai T, Saito Y, Matsuo M, Kawasaki K. ISIJ Int 1991;31:86.
[18] Furubayashi E. Scripta Metall Mater 1992;27:1493.
[19] Mishin OV, Huang X, Bowen JR, Juul Jensen D. In: Proc. of the 22nd RISØ Int. Symp. on Mater. Sci. RISØ National Laboratory, Roskilde, Denmark. 2001. p. 335.
[20] Tsuji N, Ueji R, Ito Y, Saito Y. In: Proc. of the 21st RISØ Int. Symp. on Mater. Sci. RISØ National Laboratory, Roskilde, Denmark. 2000. p. 607.
[21] Utsunomiya H, Tanda K, Saito Y, Sakai T, Tsuji N. J Jpn Soc Technol Plas 1999;40:1187.
[22] Lee SH, Saito Y, Tsuji N, Utsunomiya H, Sakai T. Scripta Mater 2002;46:281.
[23] Hansen N. Metall Mater Trans A 2001;32A:2917.